

Particles Acceleration in Converged Two Shocks

Xin Wang^{1,2,3,4,5} Joe Giacalone² Yihua Yan³ Mingde Ding⁴ Na Wang^{1,5} Hao Shan^{1,5}

1, Xinjiang Astronomical Observatory, Chinese Academy of Sciences, Urumqi 830011, China

2, Lunar and Planetary Laboratory, University of Arizona, Tucson AZ 85721, American

3, Key Laboratory of Solar Activities, National Astronomical Observatories, Chinese Academy of Sciences, Beijing 100012, China

4, Key Laboratory of Modern Astronomy and Astrophysics (Nanjing University) Ministry of Education, Nanjing 210093, China

5, Key Laboratory of Radio Astronomy, Chinese Academy of Sciences, Nanjing 210008, China

e-mail: wangxin@xao.ac.cn

ABSTRACT

Observations show that there is a proton spectral “break” with E_{break} at 1-10 MeV in some large CME-driven shocks. Theoretical model usually attribute this phenomenon to a diffusive shock acceleration. However, the underlying physics of the shock acceleration still remains uncertain. Although previous numerical models can hardly predict this “break” due to either high computational expense or shortcomings of current models, the present paper focuses on simulating this energy spectrum in converged two shocks by Monte Carlo numerical method. Considering the Dec 13 2006 CME-driven shock interaction with an Earth bow shock, we examine whether the energy spectral “break” could occur on an interaction between two shocks. As result, we indeed obtain the maximum proton energy up to 10 MeV, which is the premise to investigate the existence of the energy spectral “break”. Unexpectedly, we further find a proton spectral “break” appears distinctly at the energy ~ 5 MeV.

Subject headings: acceleration of particles—methods:numerical—shock waves—solar wind—Sun:coronal mass ejections(CMEs)

⁰* This work is supported by the Xinjiang Natural Science Foundation No. 2014211A069

1. Introduction

Diffusive shock acceleration (DSA) is regarded as the most efficient mechanism for galactic cosmic rays (CR). In the recent years several in situ observations indicate the supernova remnants (SNRs) are the essential candidates for the sources of the CR’s proton spectrum up to the “knee” at a few PeV. Since the TeV γ -ray from Crab Nebula were first clearly detected by imaging air Cherenkov telescope (IACT) in 1989, IACTs have been extensively constructed and are operating around the world. There are about one hundred γ -ray sources are identified up to now (Amenomori et al. 2009). Among of those sources, IC443 and W44 are the highest-significance SNRs in the second Fermi-LAT suited for a detailed study of their γ -ray spectra. IC443 and W44 are located at distances of 1.5kpc and 2.9kpc, respectively. Their GeV γ -ray spectra with high-energy breaks at 20GeV and 2GeV for IC443 and W44 can trace the parent protons escaped from SNRs shock and collided with the nearby molecular clouds (MCs). In addition, both the γ -ray emissions with a low-energy break at $\sim 200\text{MeV}$ also can be interpreted by effect of pion bump between SNRs protons and the MCs (i.e. $p+p \rightarrow \text{He}+\pi^0$, $\pi^0 \rightarrow 2\gamma$) (Ackermann et al. 2013). This γ -ray luminosity model can be used to explain the CRs energy spectral “break”.

In the interplanetary (IP) space, there are also find the similar energy spectral “break” in the IP shocks. There are six events with hard energy spectra occurred on Nov. 6, 97, Feb. 15, 01, Jan. 20, 05, Sep. 7, 05, Dec. 5, 06, and Dec. 13, 06. These six large events all have spectral “breaks” at the energy range of $\sim 1\text{-}10\text{MeV}$ (Mewaldt et al. 2008). In addition, there are the six largest events on the solar cycle 23 list as Jul. 14, 00, Nov. 8, 00, Sep. 24, 01, Nov. 04, 01, Nov. 22, 01, Oct. 28, 03. These events all have spectra that roll over in similar fashion beyond $\sim 50\text{MeV}$. In present paper, we discuss the Dec. 13, 06 event, which proton fluxes are based on spacecraft of ACE, STEREO, and SAMPEX.

Although a number of in situ observations exhibit the CR’s proton spectral “break” associated with either galaxy source or solar source, there is still no reliable prediction of this “break” by numerical methods. According to the theoretic model of DSA, CR’s power-law spectrum span a very large energy range from 1KeV to a few 100EeV ($\sim 10^{20}\text{eV}$). If one plans to simulate the total CR’s energy spectrum, it’s very hard for performing so expensive computer program. In addition, numerical simulation is usual to built a simple DSA model with a short size of the diffusive region ahead of shock. If the energy spectral “break” associated with a large diffusive size, the simple numerical models would hardly include this energy spectral “break” in their simulation results. Monte Carlo (MC) method can easily treat thermal ion injection (Wang et al. 2011, 2013). In MC method, the scattering mean free path is assumed to be some function of the particle rigidity, so this treatment is able to follow the evolution of individual ions long enough to model acceleration to high energies. However, the acceleration efficiency, as well as the maximum particle energy, are limited by the finite size of the accelerating region as parameterized by the free escape boundary

(FEB). Vladimirov et al. (2008) describes the escape of particles from the SNR shock with an assumed FEB far upstream of the shock. The distance to the FEB is a free parameter of the simulation that controls the maximum energy of accelerated particles and the escaping CR flux. Ellison et al. (1990) presented an ion spectra with a maximum particle energy no more than 1 MeV by applying an fixed FEB ahead of the bow shock. Knerr et al. (1996) and Wang et al. (2012) forward the maximum particle energy achieving to ~ 4 MeV by applying a moving FEB with the shock. Wang et al. (2015) investigated that the maximum particle energy limited in FEB can achieve a saturation at ~ 5.5 MeV using different scattering mean free path functions.

Since the cosmic rays are important both dynamically and diagnostically it is essential that we understand their acceleration, transport, radiative emissions, and interaction with other components of astrophysical environments. In particular, the CRs spectrum shape is usually referred to as a knee-ankle structure with the “knee” at a few PeV and the “ankle” at a few EeV. Similarly, the IP shock energy spectrum with a “break” at a few MeV. There are some debated understandings for the energy spectral “break”. One of these understandings has ever proposed that the “break” determined by the Larmor radius for ions. A heavy nucleus with charge Z has maximum energies Z times higher than a proton with same Larmor radius. However, the CRs consist mainly of protons with smaller numbers of other nuclei (Bell 2013). Another point argues that this “break” can probably be associated with the leakage mechanism. The CRs drive Alfvén waves efficiently enough to build a transport barrier that strongly reduces the leakage leading a spectral “break” (Malkov et al. 2013). Although the turbulent field exist a limited boundary, it would not be the main reason for producing the energy spectral “break”. According to the DSA, the turbulent field in the precursor is generated by the gradient of CRs pressure, which is faded gradually but not steeply. However, if a SNR shock approaches a MCs or a pre-supernova swept-up shell with a significant amount of neutrals, confinement of accelerated particles deteriorates. This would lead to a energy spectral “break” (see review in Bykov et al. 2013). In addition, there is a multiple shocks model proposed by Schneider (1993); Melrose & Pope. (1993). It is assumed that the medium is highly turbulent and that the number of shocks are propagating through it. CRs particles are injected into the system and accelerated by one or more shocks before they escaped from the system. This model may also used to study the particle spectral features such as “breaks”. In present paper, we propose that a new collided shocks model could probably inform the energy spectral “break” in the interacted precursor regions.

How to directly follow the higher energy spectral “tail” for understanding the “break” is posing a challenge to the numerical methods. Present work treats the interaction of CME-drive shock with the Earth bow shock to try investigate the energy spectral “break” as described in the observed Dec 13 2006 event. In converged two shocks, we apply the Monte Carlo simulation method without FEB. There are two reasons make it is possible to verify the spectral “break”. Firstly, the double shocks can provide enough energy injection to produce the required highest energy “tail”.

Secondly, due to no FEB, the accelerated particles can freely interact between double shocks and renew the standard DSA power-law shape.

In present paper, we do simulations to further investigate the energy spectrum in converged two shocks by using Monte Carlo method. In section 2, we introduce the converged shocks model specifically. In section 3, the simulated results and analysis are presented. In the last section, we give summaries and conclusions.

2. Model

Halo CMEs were observed by the SOHO/LASCO coronagraphs in association with the events of 13 December 2006, with speeds of 1774km s^{-1} . The flux spectra of protons in the SEP event by ACE, STEREO, and SAMPEX instruments show a “break” at $\sim 1\text{-}10\text{MeV}$. Spectra from GOES-11 also agree over the region from 5MeV to 100MeV . Although the broken spectra would be little debated due to system errors from multiple spacecraft, it is hard to obtain a completely spectra for a large energy span from an individual spacecraft. So we hopefully do a simulation to obtain an entire spectra, which can cover the energy range from thermal energy below $\sim 0.1\text{MeV}$ to superthermal energy beyond $\sim 10\text{MeV}$.

Fig. 1 shows a schematic diagram of the converged shocks model. The left reflective wall represents a CME, which produces a shock by a bulk flow speed of u_0_2 . The right reflective wall represents the Earth, which informs a bow shock by an opposite bulk flow speed of u_0_1 . Their relative speed between two bulk flows is equal to $u = |u_0_1| + |u_0_2|$, which can equivalently be taken as the relative movement between two reflective walls with opposite velocities u_0_1 , u_0_2 in the laboratory reference frame. Similarly, we can take both downstream bulk flow speeds with the same velocity zero in the laboratory reference frame. This model describes the double shocks interaction occurred on the 13 December 2006 nearby Earth. According to the Wind magnetic cloud list, the cloud axis direction is $\theta=27^\circ$, $\phi=85^\circ$ in GSE coordinates (Liu et al. 2008). In this model, we define the bulk flow direction to the interplanetary magnetic field (IMF) direction with an oblique factor of $\cos(\theta)$. So we take the relative speed between two bulk flows as value for $\sim 1600\text{km s}^{-1}$ aligned to the IMF. Both two shocks are produced by the same bulk flow speed value for $|u_0_1| = |u_0_2| = \sim 800\text{km s}^{-1}$, but with opposite direction in the laboratory frame. Also both two reflective walls produce shocks propagating with opposite velocities of v_{sh1} and v_{sh2} , respectively.

In this Monte Carlo method, we apply an initial number density of particles n_0 obeying a Maxwellian distribution with a random thermal velocity v_0 in the unshocked upstream region. Initial particles with their upstream bulk flow speeds move to their corresponding reflective walls in the both sides of the simulation box. Each bulk flow is reflected and forms the higher shocked

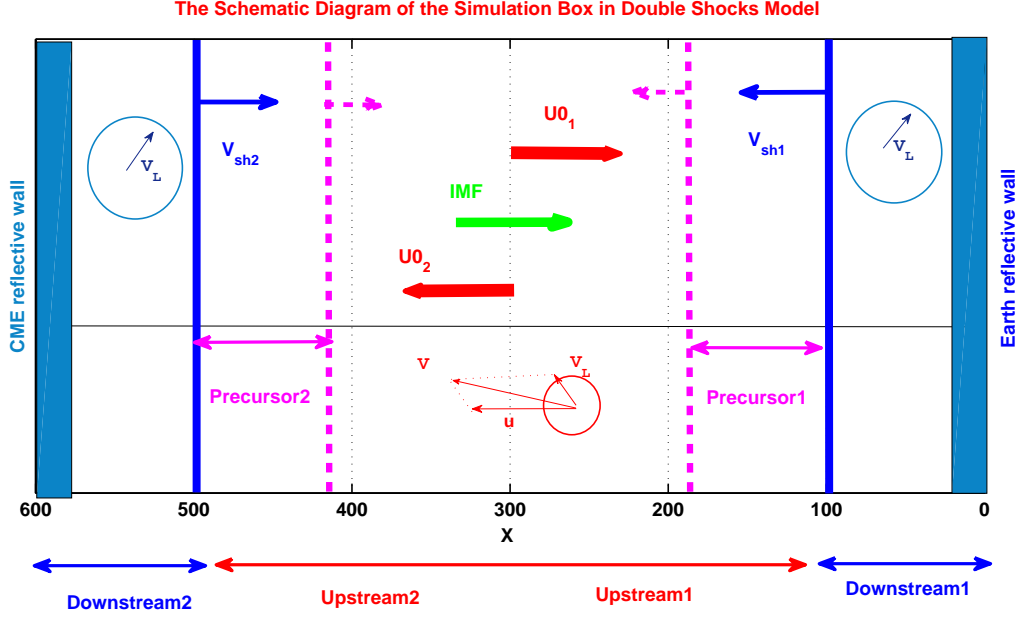


Fig. 1.— A schematic diagram of the simulation box. The left reflective wall represents a CME and produces one shock propagating from the left boundary to the middle of the simulation box. The right reflective wall represents the Earth and produces another shock involuting from the right boundary to the middle of the simulation box. Particles diffuse in the precursor regions between two shock fronts when they approach together near the middle of the simulation box.

densities as downstream region in each side of the simulation box. With the downstream density achieving to a saturation, the shock fronts smoothly evolve forward to the middle of the box with shock velocity V_{sh1} and V_{sh2} , respectively. When the two shock fronts propagate more and more close, then the two precursors have an interaction with the time at the middle of the simulation box. It is this processes the particles are able to gain their additional energies by crossing two shock fronts. Unlike previous single shock model, FEB is not included in the front of the converged two shocks. Due to the two reflective walls in this model can play a role on preventing the particles from escaping, this can ensure the particles in upstream region have enough opportunities of scattering on double shocks to obtain more energy gains. In this way, we can obtain the maximum particle energy beyond 10MeV to investigate the energy spectral “break” between 1-10MeV.

In this simulation box, the continuous bulk flow from the middle of the box with opposite directions enter into the box along to the two boundaries of the simulation box. One bulk flow forms a CME shock in the left boundary, another bulk flow forms a bow shock on the right boundary.

With the shock formations, the particles are accelerated from each shock front. With the shock propagations forwarding to the middle of the box, the precursor regions are mixed. This interaction of the precursor regions ahead of two shocks make the energetic particles either re-accelerate or de-accelerate at the end of the simulation. It is this double effect of the energetic particles is responsible to the formation of the energy spectral “break” at the range of 1MeV-10MeV.

In technically, the hybrid simulation method solves the equation explicitly for particle motions in an electromagnetic plasma (Giacalone et al. 1993; Guo et al. 2013). But the Monte Carlo method applies the scattering law for the particles diffusive processes. According to the particles mean free path (mfp) equal to the local velocity times the scattering time (i.e. $\lambda = v_l \cdot \tau$), we determine the scattering probabilities of particles based on the rate of the time step over the scattering time (i.e. $\eta = dt/\tau$). So we can chose the numbers of the particles at a certain density in each grid to diffuse with their random pitch angle deflections. By means of these diffusive processes, the particles in upstream region transfer their kinetic energy into their random thermal energy in the downstream region. Then the minority of these random thermal particles can diffuse back shock front by multiple scattering cycles to obtain more energy gains to produce the superthermal energy “tail”.

The simulation parameters mainly include upstream bulk speeds of $u0_1=-0.6$, and $u0_2=0.6$, the total size of the box $X_{max}=600$, total simulation time $T_{max}=2400$, the number of grids $n_x=1200$, the initial density per grid $n_0=360$, the constant of the scattering time $\tau_0=25/30$, initial thermal velocity $v_0 = 0.02$, and time step $dt=1/15$. The above dimensionless values are all scaled by a group of the standard scaled factors: $x_{scale}=2000R_e/600$, $t_{scale}=630'/2400$, and $u_{scale}=800\text{kms}^{-1}/0.6$, where the R_e is the Earth radius. The total number of the particles in simulation box amounts to more than 1,000,000 particles.

3. Results

3.1. Shock Evolution

The total simulation time $T_{max}=2400$ are divided into 10 periods of time represented by $Q=1, 2, 3...10$ sequently. Fig.2 shows a group of bulk flow velocity snapshots in sequence of $Q=3,5,7$ and density snapshots in sequence of $Q=2, 4, 8$. In the top panel, the bulk flow velocity with initial $u0_1$ and $u0_2$ in the upstream region evolve into the downstream with bulk flow speed of zero. From the $Q=3, 5$, to 7 , the downstream region extend from the both boundaries to the center of the simulation box. Two shock fronts propagate from the both boundaries to the center of the box with opposite shock velocities v_{sh1} and v_{sh2} , symmetrically. In front of the shocks, the velocity profiles have gradual slopes, which represent the shock precursors caused by the energetic particles

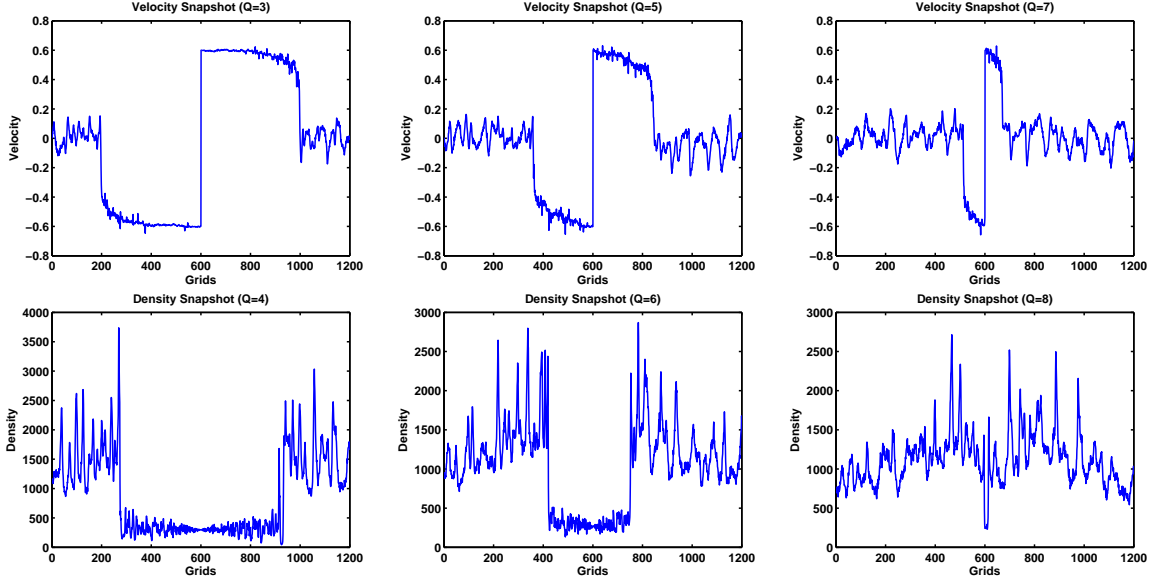


Fig. 2.— The top panel represents snapshots of the bulk flow velocity at the periods of simulation time $Q=3, 5, 7$. The low panel represents snapshots of the flow density at the periods of simulation time $Q=4, 6, 8$.

back-reaction on the shock. When the two shock fronts approach more and more close, the two precursors overlap and have an interaction between the energetic particles extracted from the both downstream regions. This interaction process may vary the regular energy spectrum. In the low panel, the bulk flow density with an initial number density n_0 per grid evolve into downstream region with a higher density. The downstream region show a higher density with several times of that in the upstream region. Noted that both downstream regions have little lower densities in time period of $Q=8$ than $Q=6$ and 4 , because our simulation model applying an adapter density with the simulation time. For the simply computation, we apply a temporally density with a reduction of density $dn=16$ in each period of time Q (i.e. adapter density reduce 1 particle from initial density n_0 per 15 simulation time units). Similarly, the density profiles can also produce an interaction on both precursor regions when the two shocks become close enough. This may induce the precursor energy spectrum with the same spectrum in the downstream region at the end of the simulation.

Fig.3 shows a group of the bulk flow velocity profiles at the periods of $Q=3, 5, 7$ and density profiles at the periods of $Q=4, 6, 8$. Top panel shows a series of the bulk flow velocity profiles in the position with the time. In the laboratory reference frame, the bulk flow velocity in both of the downstream regions are equal to zero, the bulk flow velocities in two upstream regions show an opposite movement in the middle of simulation box. The solid lines in both upstream regions represent the precursor position, respectively. The top right mesh plot shows the two precursor regions overlapping with time. This overlapping processes play two roles on the energetic particles:

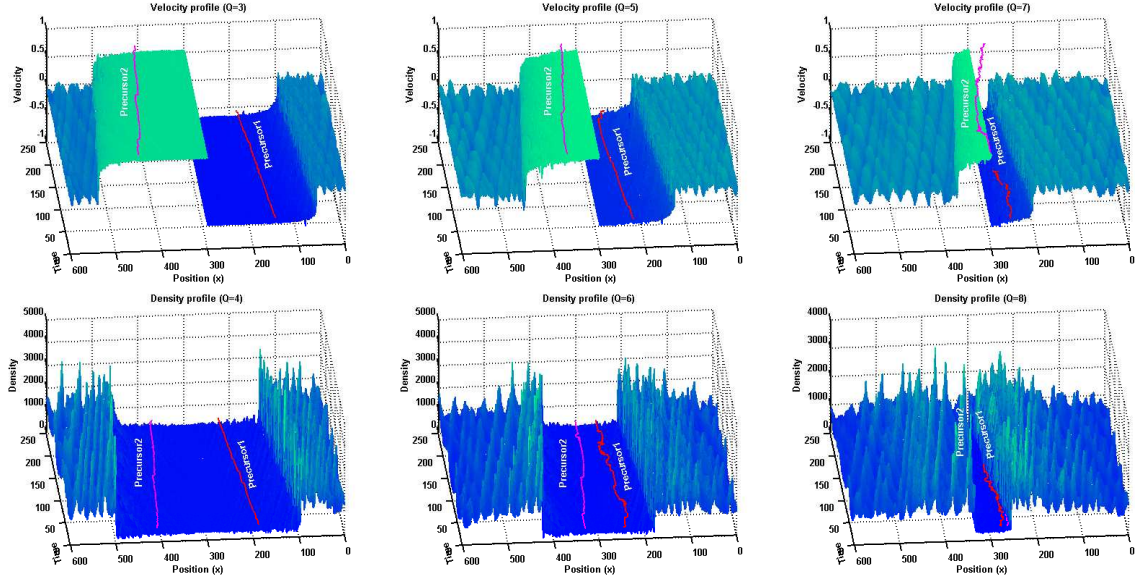


Fig. 3.— The top panel represents profiles of the bulk flow velocity at the periods of simulation time $Q=3,5,7$. The low panel represents profiles of the bulk flow density at the periods of simulation time $Q=4,6,8$.

(i) shock 2 with a positive precursor bulk velocity decelerate the energetic particles jumped from shock 1 with a negative precursor bulk velocity. (ii) In the contrary, shock 1 with a negative precursor bulk flow velocity re-accelerate the energetic particles dropped from shock 2 with a positive precursor bulk flow velocity. Lower panel shows a series of density profiles in the position with the time. The three mesh plots indicate the higher density in the downstream regions shorten the upstream regions with a lower density from the periods of $Q=4, 6$, to 8 . The right plot shows two precursor regions are mixed together with a hybrid density.

3.2. Particle Acceleration

Fig.4 shows a group of particle acceleration processes in periods of $Q=5, 6, 7, 8, 9$, and 10 . There are a part of particles extracted from the total simulation box in corresponding plot. In each pot, two triangle shadow areas represent the two shock fronts. Some of particles rotating in each shock front trace their trajectories with energy gains from the lower velocity to the higher velocity due to multiple scattering cycles on each shock front. Another particles in the downstream regions indicate they have no energy gains without velocity increasing. Maximum particle velocities V_{max} denoted with values for $31.3898, 33.5277, 35.4340, 37.3926, 37.5091$, and 36.4455 are calculated in periods of time $Q=5, 6, 7, 8, 9$, and 10 , respectively. These maximum velocities show that these particles keep accelerating with the time to achieve an saturation at a certain time, then they exhibit

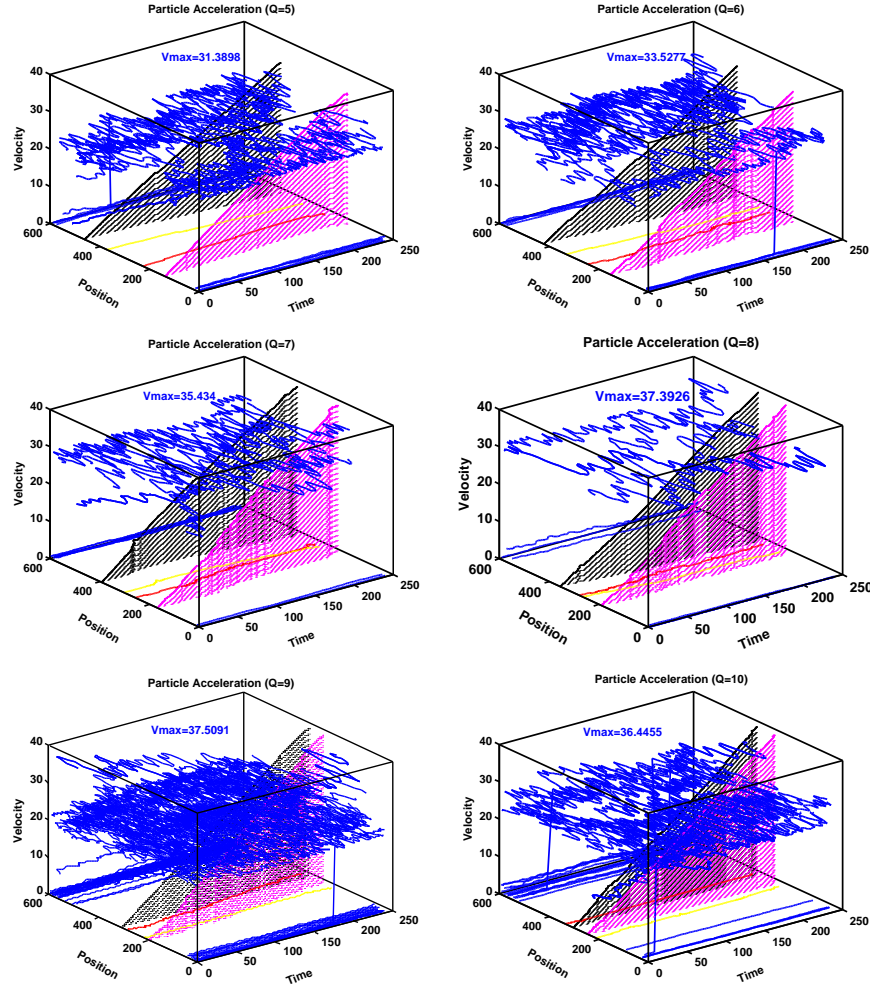


Fig. 4.— This group of plots represent particles acceleration in double shocks at the periods of simulation time $Q=5, 6, 7, 8, 9$, and 10 . These curves in each plot represent particle trajectories. These trajectories show local velocity evolutions of those particles with position and time.

deceleration processes at the end of the simulation. In the periods of time between $Q=8$ and $Q=9$, two opposite shock fronts approach more close enough, it make the energetic particles produced by one shock cross into another shock each other. Simultaneously, these two precursor regions can make the energetic particles mixing in a hybrid precursor region. Because there exist two different modifications of the precursor bulk flow velocities, the energetic particles produced by one shock region may induce either deceleration or re-acceleration in another shock region. These mixture may break a smooth single energy spectral power law followed by a single shock model.

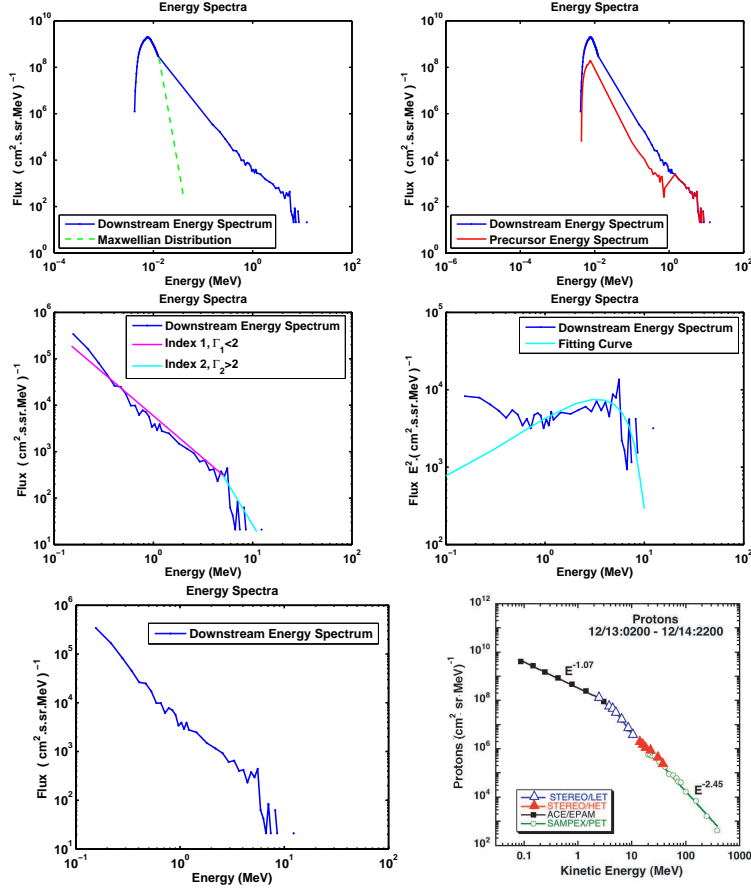


Fig. 5.— In top left plot, the solid line represents the proton spectrum with a “break” power law obtained from the downstream region at the end of simulation, the dashed line represents the thermal distribution in downstream region. In top right plot, the red line shows energy spectrum in the precursor region; the blue line shows energy spectrum in the downstream region. The middle left plot is the higher energy part of the top left plot. The pink line and cyan line show an energy spectral “break” at ~ 5 MeV. The middle right plot also indicates double energy spectral indices. Cyan curve fitted the simulation data shows one index in lower energy range is less than 2, and another index in higher energy range is more than 2. The low left plot shows the energy spectra in downstream region purely with comparison of observed spectrum from the multiple spacecraft. The flux in left plot is statistic in per second, it is consist with the flux of the right plot in period of time 44 hours.

3.3. Energy Spectra

Fig.5 shows a group of proton spectra calculated from simulation box at the end of the simulation. Each plot shows an energy spectral “break” at ~ 5 MeV. The blue curve in top left plot represents the energy spectrum with a Maxwellian peak at a few keV and with an extended power law energy spectral “tail” in downstream region. The energy spectral “break” occurs at the energy of ~ 5 MeV. The dashed line indicates the potential Maxwellian distribution in the shocked downstream. The top right plot represents two energy spectra in upstream and downstream regions, respectively. The pink color curve denotes the energy spectrum in upstream region and the blue color curve denotes the energy spectrum in downstream region. From the energy range of ~ 1 MeV to ~ 10 MeV, the energy spectrum in upstream region with the same shape of the energy spectrum in downstream. Both of them appear energy spectral “breaks” at ~ 5 MeV. For convenience to

study the energy spectral “break”, we extract a part of energy spectrum from the total downstream energy spectrum as shown in the middle left plot. The pink line represents the harder energy spectrum with an index less than 2, and the cyan line represents the softer energy spectrum with an index more than 2. The “break” indicate that there exist a double power law spectrum. The middle right plot gives an energy spectral shape in the flux of $E^2 \cdot F(E)$ representation, in which the lower energy spectrum exhibits a descent slope shape, and the higher energy spectrum exhibits a dropped slope shape. The fitting curve clearly shows that there exist a double power-law with a “break” at $\sim 5\text{MeV}$. The low panel presents a comparison of the simulated energy spectrum with the observed energy spectrum. The low left plot is the simulated energy spectrum in the downstream region purely; the low right plot is the observed energy spectrum in the downstream region too (Mewaldt et al. 2008). The difference of the flux between two energy spectra is caused by different integrating time. The simulated flux is integrated in one second, but the observed flux is the sum of the period from 2006 Dec 13, 02:00 to Dec 14, 22:00, which is equivalent to $1.584 \times 10^5\text{s}$. So the simulated and the observed fluxes are well agreement in the normalized time.

4. Summaries and Conclusions

In summary, we do simulation of the converged two shocks for obtaining the proton spectrum directly. Comparing with the observed energy spectrum from multiple spacecraft. Simulated energy spectrum exhibits the consist “break” at the energy $\sim 5\text{MeV}$. Although the numerical computation is very expensive, we obtain the highest energy spectral “tail” up to $\sim 10\text{MeV}$. We have updated the results of the maximum particle energy, which can not predict the energy spectral “break” in a single shock model. Why the previous efforts can not predict the energy spectral “break” ? There would be two reasons: (i) the single shock model can not provide enough energy to transfer the energetic particles to the highest energy up to $\sim 10\text{MeV}$. (ii) The shortage of the interaction mechanism make it impossible to re-accelerate or decelerate the energetic particles. However, the converged shocks model can satisfy these two essential conditions. Firstly, the converged shocks model can provide enough energy injection than a single shock model to produce the highest energy spectral “tail”. Secondly, it can also provide an interaction mechanism to break the standard single power law energy spectrum formed by a single shock model. In converged two shocks, those energetic particles produced in each individual shock can mix together into the hybrid precursor region when two shocks approach more and more close. It is just these opposite precursor bulk flow velocities present the variation of the energetic particles distribution and produce an energy spectral “break” at the higher energy tail.

Present work is supported by Xinjiang Natural Science Foundation No. 2014211A069. This work is also funded by CAS grant KLSA201511, the Key Laboratory of Modern Astronomy and Astrophysics (Nanjing University), Ministry of Education, and China Scholarship Council (CSC). Simultaneously, authors thank the support from Supercomputer Center of University of Arizona. In addition, authors are also appreciate Profs. Hongbo Hu and Hong Lu in Institute of High Energy Physics of Chinese Academy of Sciences for their many helpful discussions.

REFERENCES

- Ackermann, M., et al, 2013, *Science*, **339**, 807-811
- Amenomori, M., et al, 2009, *ApJ*, **692**, 61-72
- Bell, A. R., 2013, *Astroparticles Physics*, **43**, 56-70
- Bykov, A. M., Malkov, M. A., Raymond, J. C. & et al., 2013, *Space Sci. Rev.*, **178**, 599-632.
- Ellison, D. C., Möbius, E. & Paschmann, G. ,1990, *ApJ*, **352**, 376-394
- Giacalone, J., Burgess, D., Schwartz, S. J., & Ellison, D. C., 1993, *ApJ*, **402**, 550-559
- Guo, F., & Giacalone, J., 2013, *ApJ* , **773**, 158
- Knerr, J. M., Jokipii, J. R. & Ellison, D. C., 1996, *ApJ* , **458**, 641-652
- Liu, Y., Luhmann, J. G., Müller-Mellin, R., et al., 2008, *ApJ* , **689**, 563.
- Malkov, M. A., Diamond, P. H., & et al, 2013, *ApJ*, **768**, 73-85
- Melrose, D. B., & Pope, M. H., 1993, *Proceedings of the Astron. Soci. Austr.*, **10(3)**, 222.
- Mewaldt, R. A., et al. ,2008, *Proceedings of the 30th ICRC(Mexico)* , **1**, 107-110.
- Schneider, P., 1993, *Astron. Astrophys.*, **278**, 315-327
- Vladimirov, A., Bykov, A., & Ellison, D. C., 2008, *ApJ*, **688**, 1084-1101
- Wang, X. et al., 2013, *ApJS* , **209**, 18
- Wang, X. et al., 2011, *Astron. Astrophys.*, **530**, A92
- Wang, X. et al., 2012, *Res. Astron. Astrophys.*, **12**, 1535-1548
- Wang, X. et al., 2015, *Res. Astron. Astrophys.*, <http://arxiv.org/abs/1509.04182>